Oceanographic dynamics and the end of the last interglacial in the subpolar North Atlantic

Zohra Mokeddem[a,1,2], Jerry F. McManus[a], and Delia W. Oppo[b]

[a]Lamont-Doherty Earth Observatory, Columbia University, Palisades, NY 10964; and [b]Department of Geology and Geophysics, Woods Hole Oceanographic Institution, Woods Hole, MA 02543

Edited by James P. Kennett, University of California, Santa Barbara, CA, and approved June 19, 2014 (received for review November 27, 2013)

The last interglacial interval was terminated by the inception of a long, progressive glaciation that is attributed to astronomically influenced changes in the seasonal distribution of sunlight over the earth. However, the feedbacks, internal dynamics, and global teleconnections associated with declining northern summer insolation remain incompletely understood. Here we show that a crucial early step in glacial inception involves the weakening of the subpolar gyre (SPG) circulation of the North Atlantic Ocean. Detailed new records of microfossil foraminifera abundance and stable isotope ratios in deep sea sediments from Ocean Drilling Program site 984 south of Iceland reveal repeated, progressive cold water-mass expansions into subpolar latitudes during the last peak interglacial interval, marine isotope substage 5e. These movements are expressed as a sequence of progressively extensive southward advances and subsequent retreats of a hydrographic boundary that may have been analogous to the modern Arctic front, and associated with rapid changes in the strength of the SPG. This persistent millennial-scale oceanographic oscillation accompanied a long-term cooling trend at a time of slowly declining northern summer insolation, providing an early link in the propagation of those insolation changes globally, and resulting in a rapid transition from extensive regional warmth to the dramatic instability of the subsequent ~100 ka.

gyre systems | cold anomalies | frontal zone | ocean circulation

The last peak interglacial, marine isotope substage (MIS 5e), reached globally warmer conditions than modern conditions (1–3) before giving way to the extreme conditions and instability of the subsequent ice age. Although the process of glacial inception is not fully understood, it is generally considered to be paced by the external influence of declining northern summer insolation (4, 5), and associated with internal processes such as atmospheric CO_2 decline (6). The global transmission and amplification of the declining northern insolation require internal mechanisms that link the early response of the high northern latitudes (5, 7) with the rest of the globe. Ocean circulation is a likely candidate to play this role (5) with both the surface and shallow circulation of currents, fronts, and gyre systems (8, 9), as well as the deeper overturning circulation (10, 11), serving as crucial links in the chain of global teleconnections. It has also been suggested that millennial climate oscillations of the last climate cycle (12) were initially limited to the high-latitude North Atlantic before extending globally (13), which underscores the importance of documenting the early response in these regional systems. Recent efforts have allowed the reconstruction of the last interglacial conditions on Greenland from deformed ice (3), and Greenland climate can also be inferred using Antarctic ice cores, assuming a bipolar seesaw pattern (14). Nevertheless, the millennial-scale regional oceanographic variability of the last interglacial is best captured in deep sea sediment cores (15–19).

The North Atlantic subpolar gyre plays a particularly important role in the climate system, and shares links with the Nordic seas and Arctic Ocean through the surface transport and exchange of heat, salinity, and freshwater (20, 21). It also helps modulate the production of deep and intermediate waters via convection in the Labrador and Nordic seas, and consequently influences the regionally and globally important Atlantic Meridional Overturning Circulation (AMOC; refs. 21, 22). The gyre circulation serves as a valuable setting for predicting regional climate variability on yearly to decadal timescales (23, 24). Understanding the behavior of the SPG during past climate change is therefore likely to provide insights into its potential role in modern and future variability.

Previous observations suggest that a continued transport of warmer and saltier water to the high northern latitudes by the AMOC provided a moisture source for ice-sheet growth during the transition from MIS 5e to the subsequent glacial substage, MIS 5d (17, 25, 26). Ocean models provide some support for this potential connection (19, 27, 28) although they disagree about whether the AMOC was strengthened (27) or merely persistent (28, 29) during the glacial inception. The influence of ocean circulation on glacial growth may have been particularly effective in the subpolar latitudes of the North Atlantic, where major ice sheets expanded, as some studies have instead ascribed the additional glacial growth at very high latitudes in Scandinavia to changes in surface ocean circulation that allowed proximal cooling (30).

Recent studies have demonstrated the influence of the subpolar oceanographic–atmospheric system on the properties of the modern North Atlantic Current (NAC) and its transport of heat, salt, and moisture to the highest latitude North Atlantic (20, 22, 31). The northeast and main branch of the NAC is drawn primarily from the subtropical gyre (STG), and becomes warmer and saltier when the SPG circulation weakens (22) as a consequence of either a weakening of the westerlies (22, 32) or enhanced

Significance

The last interglacial, ~125,000 y ago, was the last extended warm period the earth has known before our Common Era of the past 11,000 y. Its end came after ~15,000 y, paced by the decline in northern summer insolation, and followed by a glacial age lasting 100,000 y. Yet the ocean dynamics contributing to this glacial initiation and its global propagation are not fully understood, nor are their general role in climate evolution understood. This study assesses the role of the ocean's gyre systems and fronts as dynamical components in large-scale climate change. Using microfossils, we document progressive southward advances of Arctic and polar hydrographic fronts into the subpolar North Atlantic Ocean, which trigger regional coolings and accelerate the transition into the glacial age.

Author contributions: Z.M. and J.F.M. designed research; Z.M. and J.F.M. performed research; J.F.M. and D.W.O. contributed new reagents/analytic tools; and Z.M., J.F.M., and D.W.O. wrote the paper.

The authors declare no conflict of interest.

This article is a PNAS Direct Submission.

[1]Present address: Institut Français de la Recherche pour l'Exploitation de la Mer, Centre de Bretagne, 29280 Plouzané, France.

[2]To whom correspondence should be addressed. Email: mokeddem@ldeo.columbia.edu.

This article contains supporting information online at www.pnas.org/lookup/suppl/doi:10.1073/pnas.1322103111/-/DCSupplemental.

cold and fresh water outflow brought by the East Greenland Current into the subpolar northwest Atlantic (Fig. 1). At these times, water masses with subtropical properties are preferentially conveyed toward the northeast Atlantic and into the Nordic seas over the Greenland–Scotland Ridge (8, 20, 22). In contrast, during the episodes of SPG strengthening, the warm and salty subtropical water masses flowing northeast are split and shared with the Irminger Current (IC) that flows southwest of Iceland, serving as both the westward branch of the NAC and northern branch of the SPG. In the SPG-weakening configuration, deep ocean convection slows down in the Labrador Sea in the northwestern Atlantic (21, 33), while the enhanced flow of warm and salty surface water to the northeast contributes to persistent deep water formation in the Nordic seas (34), as is also evident in model simulations of the last interglacial MIS 5e (8).

In this study, we use deep sea sedimentary records to reconstruct oscillations that involve the strengthening and weakening of the SPG and the repeated migration of the Arctic front (AF) and polar front (PF) during the last interglacial period and subsequent glacial inception. We adopt the definition of the AF as being the boundary separating the Arctic and Atlantic domains and the PF as the limit between the polar and Arctic domains (35). The data include detailed sedimentary and isotopic analyses and are based on scenarios of the AF and PF movements and the northwest contraction of the SPG that have been proposed for both interglacial and glacial settings (36–38). A series of increasingly extensive advances and diminishing retreats of these oceanographic frontal zones culminated in the glacial inception when the AF fully entered the subpolar North Atlantic, blocking heat transport to the entire northwest Atlantic (1, 17) and initiating the global sequence of rapid, hemispherically out-of-phase climate variability that characterized the last ice age (1, 13). However, paradoxically, the repeated increases of heat and moisture flux to high latitudes in the northeast Atlantic may have contributed to enhanced ice growth (17, 25) and the end of the MIS 5e peak interglacial interval.

Results

Our investigations are based on new results from Ocean Drilling Project (ODP) site 984 south of Iceland (61.25°N, 24.04°W; 1,648 m) compared with existing evidence from other locations, particularly from ODP site 980 (55.49°N, 14.70°W; 2,170 m) (39, 40) situated farther southeast in the subpolar North Atlantic Ocean (39, 40) (Fig. 1). The stratigraphies for the long sedimentary sections from these two drilling sites are based on the identification of MIS 5e in the respective benthic $\delta^{18}O$ and characteristic peaks in the abundance of ice-rafted debris (IRD) that bracket MIS 5e (Fig. 2).

The oceanographic reconstructions are based on the abundances of planktonic foraminifera and IRD, planktonic and benthic stable oxygen-isotope ratios (expressed as $\delta^{18}O$), and benthic stable carbon-isotope ratios (expressed as $\delta^{13}C$). Planktonic foraminifera assemblages and $\delta^{18}O$ help establish variations in near-sea-surface environment and hydrography. Three particular indicator species were used to provide information about frontal systems. *Neogloboquadrina pachyderma*, sinistral coiling (NpS), is associated with the polar waters at high latitudes (41–43). It is the predominant foraminifera poleward of the polar front in the modern ocean, and is essentially absent equatorward of the AF (44). *Turborotalita quinqueloba* (Tq) is found in strong association with the modern AF, with sharply decreasing abundances both poleward and equatorward of the front (45, 46). In surface sediments of the modern Nordic seas, Tq abundance reaches a maximum of 45%, with a range of 10–20% north and east of Iceland, whereas the abundance range is 2–10% near our study sites (43, 44). A similar distribution characterizes the warmest intervals of this study, and the cooler intervals are reflected in coherent southward shifts of the Tq maximum abundance. *Neogloboquadrina pachyderma*, dextral coiling (NpD), is a more typical subpolar species, with a broad temperature tolerance and moderate abundances between subtropical and Arctic waters (46, 47). Sinistral and dextral coiling varieties are genetically distinct in modern *N. pachyderma*, with the exception of a small number (<3%) of individuals within the population (48). The low level of aberrant

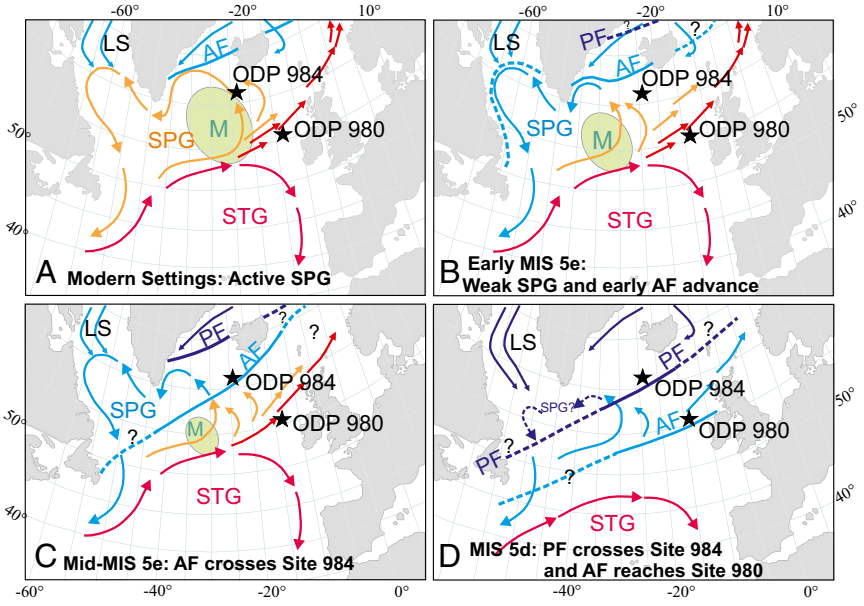

Fig. 1. Study setting in the subpolar North Atlantic Ocean with surface currents (arrows): red (warm subtropical waters), orange (cool subpolar waters), light blue (Arctic waters), and dark blue (polar waters). Dashed light and dark blue lines indicate hypothetical locations of the AF and PF. *A–C* indicate currents associated with expanded and contracted SPG and associated zones of maximal mixing (M) with STG. *B*, *C*, and *D* show contracted SPG and the advances of the AF and PF within the cold events C28 and C27, C27a and C27b, and C26 and C25, respectively. Stars indicate locations of deep sea sediment cores ODP 980 and ODP 984. LS refers to the Labrador Sea. Modern location (*A*) of the AF and PF are described by ref. 35.

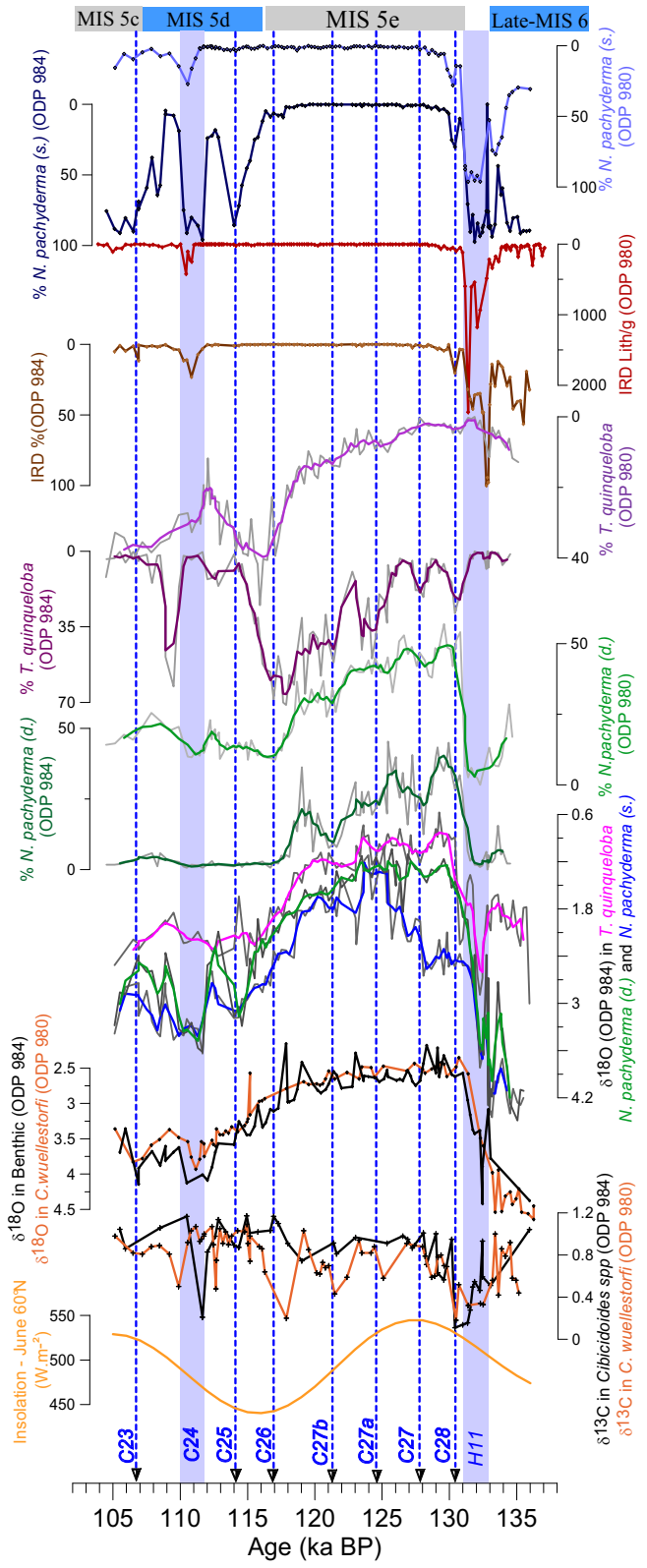

Fig. 2. Isotopic, faunal, and sedimentological data from ODP sites 980 and 984 plotted against age in kilo annum before present (ka BP). Dotted blue lines (C23 to C28) denote cold events revealed by peaks of *T. quinqueloba* abundance, previously identified by refs. 50 and 40. Summer insolation values expressed in watts per square meter ($w{\cdot}m^{-2}$) are for latitude 60°N (4). Three-point running means applied on fauna abundance and planktonic $\delta^{18}O$ plots are shown in bold.

forms lends uncertainty to interpretations of small changes (48) in the abundance of each, although not to the substantial variations of tens of percent observed in the microfossil assemblages of this study.

The polar NpS reaches a dominant abundance at both sites during the deglacial transition (Fig. 2), at the same time as the occurrence of a peak in IRD related to a major iceberg discharge, Heinrich event 11 (H11) (49). This oldest of the events identified by Heinrich (49) is evident throughout the North Atlantic (16, 17, 40, 50–52), and is recognized in associated changes globally (14, 53, 54). Immediately thereafter, NpS and IRD abundances decrease sharply, as the benthic $\delta^{18}O$ reaches its peak interglacial level and the subpolar NpD abundance rises to its maximum. Throughout MIS 5e, NpD abundances rise and fall in a series of millennial oscillations along with a generally declining trend at both sites (Fig. 2). Similarly, the abundance of all subpolar species at site 984 peaks early in MIS 5e and then generally declines along with summer insolation through the course of the peak interglacial (Fig. S1). During the same interval Tq abundances generally increase, gently at site 980, and in a series of oscillations with increasing amplitude at site 984 (Fig. 2). As benthic $\delta^{18}O$ begins to rise at ~118 ka, one last peak in NpD is followed by a synchronous peak in Tq at both sites and then a return of the polar NpS at ~114 ka at site 984. Following one more warming evident as a decrease in NpS at site 984 and Tq at site 980, the abundance of IRD and NpS increases at both sites at ~111 ka, the sea surface cooling ("C") event labeled C24 (15), as it does across much of the North Atlantic (16, 17, 50, 55). Just before this event, the benthic $\delta^{18}O$ reaches its highest values associated with the stadial substage MIS 5d.

The benthic $\delta^{18}O$ decreases to its lowest levels associated with peak interglacial conditions relatively early at ~130 ka and then increases only ~0.2‰ over the course of the subsequent 12 ka. NpD and Tq $\delta^{18}O$ similarly reach their lowest values early and then increase more sharply through the interglacial (0.4–0.8‰). Foraminifera $\delta^{18}O$ reflect a global influence of ice volume, and a local hydrographic influence of temperature and salinity including glacial meltwater, and therefore density. At our study sites, the planktonic $\delta^{18}O$ are generally ~1‰ lower than the benthic $\delta^{18}O$ during the interglacial interval (Fig. 2), although they are nearly similar, indicating diminished stratification, during the preceding glacial MIS 6 and H11 event. Of the plankton, NpS has the highest $\delta^{18}O$, reflecting its generally colder preferred environment seasonally and also its subsurface habitat (42). Tq generally has the lowest $\delta^{18}O$ throughout the record, consistent with evidence for its very shallow habitat (56). It is thus the most sensitive indicator of changes in the sea surface, and records the millennial interglacial oscillations evident in faunal abundances at both sites (Fig. 2). These oscillations in Tq $\delta^{18}O$ at site 984 are similar to millennial abundance variations at both sites, although they are less pronounced, most likely due to the combined influence of temperature and salinity, which covary in the modern ocean, yet have competing isotopic impact.

Benthic foraminifera $\delta^{13}C$ reflects the ratio of dissolved inorganic carbon of the bottom waters at each location. Values at site 984 are generally similar or higher than those of site 980, reflecting its shallower water depth and more proximal setting to the convective source regions and Nordic seas overflows. Both sites display similar overall trends throughout the study interval, with minimum $\delta^{13}C$ of 0.2–0.3‰ subsequent to the H11 event on the deglacial transition into MIS 5e, a sharp increase immediately afterward to near 0.8‰, and a general subsequent rise throughout the course of peak interglacial to near-modern values exceeding 1.0‰. A series of millennial oscillations in $\delta^{13}C$, on the order of 0.2–0.4‰, is evident throughout the study interval at site 980 (40). However these are only expressed in a subtle way, if at all, at site 984, between events C24 and H11, which are associated with significant benthic $\delta^{13}C$ decreases at both locations.

Discussion

The most prominent feature in our data for the last interglacial interval is a series of oscillations in the relative abundance and isotopic composition of the three indicator foraminifera species, indicating repeated warming and cooling of the surface ocean south of Iceland. They are too rapid to be caused by the slowly declining northern summer insolation at the time, and are more consistent with changes in the strength of the SPG and associated shifts in oceanic heat transport. These coherent, millennial-scale variations appear to reflect a balance between cold water from the north and warm from the south. The weakening of the SPG combined with the strengthening of the cold, shallow southward outflow between Greenland and Iceland may control the mean position of oceanographic frontal zones in the subpolar North Atlantic.

As an indicator of the position of the AF (46, 57), each peak of Tq abundance within MIS 5e at site 984 suggests a southward advance in the mean geographic location of the front southwest of Iceland. These observations provide robust evidence for the repeated migration of the boundary between polar from subpolar waters, although once the frontal zones entered the open North Atlantic, a similar dynamical control as inferred for the modern Nordic Seas may not apply. We associate several of these peaks of Tq abundance with a series of cool anomalies identified previously within MIS 5e (40, 52). The last Tq peak, corresponding to the C26 event, reached 70% of the population in late MIS 5e (Fig. 2), suggesting a mean location of the AF very near site 984. This cooling was more prolonged (~2 ka) than the previous ones, probably indicating an interval of significant sea-ice invasion and/or ice-sheet growth in northern latitudes. This prominent cooling also reached site 980 as indicated by the first significant rise in Tq abundance at this site (Fig. 2), and occurs as benthic $\delta^{18}O$ increases. During the subsequent event, C25, a significant increase in NpS abundance at site 984 indicates the advance of cold northern water associated with the PF near this location for the first time since the onset of the interglacial interval. After C25, both fronts briefly retreated northward but then readvanced at the time of C24, when NpS abundance increased across the subpolar region (16, 17, 55) and IRD peaked at both locations. Subsequently, the fronts continued to advance and retreat, although a peak in Tq at site 984 indicates the retreat of the AF from the North Atlantic at the transition into the interstadial MIS 5c.

The cold anomalies corresponding to the peaks of Tq abundance reflect the influence of cold Arctic water mass when the SPG weakens; whereas, the increases in the abundance of NpD reflect episodes of rising surface temperature due to greater influence of warm subtropical water mass as the SPG strengthened. At site 984, the data show a likely millennial timescale "competition" between episodes of warmer subtropical water inflow carried by IC and episodes of cold Arctic water outflow through the Greenland Current. The relative influence of these two water masses alternated on millennial timescales against a background of declining sea surface temperature south of Iceland as summer insolation declined and Arctic waters advanced. However, even as cold water outflow was increasing to the southwest of Iceland, warm and salty subtropical water mass continued its permanent flow to the northeast Atlantic from early to late MIS 5e before C26 (8, 9, 19).

AMOC and deep water formation generally remained active throughout MIS 5e, as recorded by an increasing trend in benthic $\delta^{13}C$ values at sites 980 and 984, as elsewhere in the North Atlantic (9, 11, 17, 40) and higher latitudes (18, 19). Within the peak interglacial, a series of millennial oscillations in the deeper site 980 is not evident at site 984, which most likely reflects the more limited impact of smaller interglacial oscillations in deep water formation, in contrast to the greater influence of H11, and to a lesser extent C24, on the deep circulation. Larger shifts in $\delta^{13}C$ have recently been observed within MIS 5e at a deeper site (3.4 km) south of Greenland (58). Although the inferred centennial-scale changes in deep waters at that site may not be fully defined in the millennial scale $\delta^{13}C$ record of site 984 due to absent epibenthic fauna in some intervals, the contrasting records may also be due to the longitudinal and depth differences, suggesting changes influencing the deepest waters may have originated from the Denmark Strait overflow, rather than the Iceland Sea overflow that bathes site 984. At this deeper site, as in our study, benthic $\delta^{13}C$ reached a maximum during the glacial growth of MIS 5d, indicating a return to significant, if not enhanced, AMOC during this transition until the sharp decrease associated with C24.

The observed variability at site 984 may be put into a regional context by comparison with site 980 to the south along with evidence from the Labrador Sea to the west and the Nordic seas to the north. Several cores at the southern tip of Greenland provide evidence for cool, relatively stable sea surface temperatures during MIS 5e (33, 59, 60), indicating the continuous southward flow of the East Greenland Current into the Labrador Sea. However, several oscillations are evident in the sea surface salinity of these waters (33), suggesting variability in the delivery of sea ice and meltwater by the current. Enhanced freshwater fluxes into the Labrador Sea would weaken the SPG, allowing warmer subtropical waters to penetrate farther to the northeast and into the Nordic seas. This process would stabilize the water column and further weaken convection in the Labrador Sea, which may have been minimal throughout MIS 5e (33). The injection of heat and salt into high latitudes would have a positive effect on deep water formation north of Iceland, and a negative feedback on the production and export of sea ice, eventually leading to a strengthening of the SPG, diminished inflow to the Nordic seas and a repeat of the entire cycle. Similar feedback mechanisms involving the SPG during the glacial inception are supported by model simulations (8) and the new results from site 984 indicate that repeated oscillations accompanied the general regional cooling trend associated with declining summer insolation.

Evidence from north of Iceland also reveals millennial oscillations during the study interval (57). Although the polar NpS was predominant throughout MIS 5e near Greenland, and was generally the most abundant form in the Iceland Sea, a series of peaks in Tq across this sea clearly represent modest warmings during MIS 5e. It is unlikely that these increases were coeval with the Tq peaks at site 984, because those reflected cooling south of Iceland. Instead, the oscillations in the Iceland Sea were more likely the northern expression of the same frontal migrations that reached and eventually extended southward of site 984 toward site 980 as polar waters reflected by NpS covered the Nordic seas (57) and entered the North Atlantic at the time of C24 during the glacial inception. By this time, the influence of cold polar waters reflected by increased NpS abundance was evident across the subpolar ocean (16, 17, 39, 40, 50–52, 61), the transition to the stadial substage MIS 5d was complete (17, 50), deep ocean circulation shifted (17, 51, 52, 58, 62, 63), and the millennial bipolar climate instability that prevailed throughout the subsequent 100 ky was firmly established (13).

Conclusions

Sedimentary data from the North Atlantic document a progressive series of coherent millennial advances and retreats of polar and Arctic water masses during the last peak interglacial substage MIS 5e and the ensuing transition to the earliest glacial inception. The progressive ramping up of repeated Tq peaks at site 984 south of Iceland suggests that millennial sea surface variability accompanied a longer-term trend of regional cooling associated with the decline in northern summer insolation. Advances of the AF past southern Iceland during the millennial

cold (C) events also signal the likelihood of episodic and progressive weakening and contracting of the SPG farther to the southwest throughout this same interval. The advance of the polar front south of Iceland, initially during C25 and subsequently to a greater extent during the prominent cold events C24 and C23, indicates a further southerly migration of cold surface water and sea ice. Several of the AF advances identified here within MIS 5e may also be related to cold events recorded north of Iceland (57), southwest of Greenland (59), northeast of the Labrador Sea (60), and in the eastern subpolar Atlantic (18, 40), which have been interpreted as episodes of meltwater pulses and Arctic sea-ice discharges (60) perhaps connected to a series of changes in deep water convection (58). As a consequence of freshwater input (60), the Arctic and polar fronts and water masses advanced southward, weakening the SPG and causing it to contract to the northwest. This allowed the warm and salty waters from the STG to penetrate to higher latitudes in the northeast Atlantic and into the Nordic seas (19, 64), which in turn contributed to the intensification of northern AMOC during glacial inception, as proposed by previous model and data inferences (17, 26, 27). Paradoxically, despite the northward heat transport of this inflow, the intensified deep overturning at this time may have contributed to the regional and thus global glaciation by providing a moisture source for incipient glaciers (17, 19, 65). The evidence presented here confirms the persistence of millennial variability during MIS 5e (14, 40, 59, 66) and indicates that these oscillations were superimposed on a long-term cooling trend associated with declining northern summer insolation throughout the last interglacial and leading into the glacial inception in the North Atlantic region. The variability was expressed in oceanographic changes, including a series of advances and retreats of the Arctic and polar fronts, influencing the gyre systems and overturning circulation of the North Atlantic. Each successive advance reached farther into the subpolar Atlantic before retreating, causing the SPG to weaken and contract, allowing the enhanced flow of subtropical waters to the northeast, amplifying variations in deep water production and thereby accelerating the process of ice-sheet growth initially set in motion by slowly declining insolation.

ACKNOWLEDGMENTS. We thank O. Hyams, J. Cullen, W. Curry, P. deMenocal, and M. Jeglinski for help with various stages of the project. R. Mortlock and J. Wright provided assistance with many of the study analyses at the Rutgers stable isotope laboratory. This is a contribution to the Past Global Changes (PAGES) Working Group on Past Interglacials. This research was funded in part by Schlumberger Foundation (Z.M.), and by awards from the United States National Science Foundation and Comer Science and Education Foundation (J.F.M.).

1. Landais A, et al. (2003) A tentative reconstruction of the last interglacial and glacial inception in Greenland based on new gas measurements in the Greenland Ice Core Project (GRIP) ice core. *J Geophys Res* 108(D18):4563.
2. Kopp RE, Simons FJ, Mitrovica JX, Maloof AC, Oppenheimer M (2009) Probabilistic assessment of sea level during the last interglacial stage. *Nature* 462(7275):863–867.
3. NEEM Community Members (2013) Eemian interglacial reconstructed from a Greenland folded ice core. *Nature* 493(7433):489–494.
4. Berger A, Loutre MF (1991) Insolation values for the climate of the last 10 million years. *Quat Sci Rev* 10(4):297–317.
5. Imbrie J, et al. (1992) On the structure and origin of major glaciation cycles 1. Linear responses to Milankovitch forcing. *Paleoceanography* 7(6):701–738.
6. Petit JR, et al. (1999) Climate and atmospheric history of the past 420,000 years from the Vostok ice core, Antarctica. *Nature* 399(6735):429–436.
7. Koc N, Jansen E (1994) Response of the high-latitude Northern Hemisphere to orbital climate forcing: Evidence from the Nordic Seas. *Geology* 22(6):523–526.
8. Born A, Nisancioglu KH, Risebrobakken B (2011) Late Eemian warming in the Nordic Seas as seen in proxy data and climate models. *Paleoceanography* 26(2):PA2207.
9. Cortijo E, et al. (1999) Changes in meridional temperature and salinity gradients in the North Atlantic Ocean (30°-72°N) during the last interglacial period. *Paleoceanography* 14(1):23–33.
10. Wang Z, Mysak L (2001) Ice sheet–thermohaline circulation interactions in a climate model of intermediate complexity. *J Oceanogr* 57(4):481–494.
11. Govin A, et al. (2009) Evidence for northward expansion of Antarctic Bottom Water mass in the Southern Ocean during the last glacial inception. *Paleoceanography* 24(1):PA1202.
12. Voelker AHL (2002) Global distribution of centennial-scale records for Marine Isotope Stage (MIS) 3: A database. *Quat Sci Rev* 21(10):1185–1212.
13. Capron E, et al. (2012) A global picture of the first abrupt climatic event occurring during the last glacial inception. *Geophys Res Lett* 39(15):L15703.
14. Barker S, et al. (2011) 800,000 years of abrupt climate variability. *Science* 334(6054): 347–351.
15. McManus JF, et al. (1994) High-resolution climate records from the North Atlantic during the last interglacial. *Nature* 371(6495):326–329.
16. Chapman MR, Shackleton NJ (1999) Global ice-volume fluctuations, North Atlantic ice-rafting events, and deep-ocean circulation changes between 130 and 70 ka. *Geology* 27(9):795–798.
17. McManus JF, Oppo DW, Keigwin LD, Cullen JL, Bond GC (2002) Thermohaline circulation and prolonged interglacial warmth in the North Atlantic. *Quat Res* 58(1):17–21.
18. Bauch HA, Kandiano ES (2007) Evidence for early warming and cooling in North Atlantic surface waters during the last interglacial. *Paleoceanography* 22(1):PA1201.
19. Risebrobakken B, et al. (2007) Inception of the Northern European ice sheet due to contrasting ocean and insolation forcing. *Quat Res* 67(1):128–135.
20. Häkkinen S, Rhines PB (2004) Decline of subpolar North Atlantic circulation during the 1990s. *Science* 304(5670):555–559.
21. Born A, Stocker TF (2014) Two stable equilibria of the Atlantic Subpolar Gyre. *J Phys Oceanogr* 44(1):246–264.
22. Hátún H, Sandø AB, Drange H, Hansen B, Valdimarsson H (2005) Influence of the Atlantic subpolar gyre on the thermohaline circulation. *Science* 309(5742):1841–1844.
23. Matei D, et al. (2012) Two tales of initializing decadal climate prediction experiments with the ECHAM5/MPI-OM Model. *J Clim* 25(24):8502–8523.
24. Yeager S, Karspeck A, Danabasoglu G, Tribbia J, Teng H (2012) A decadal prediction case study: Late-twentieth-century North Atlantic ocean heat content. *J Clim* 25(15): 5173–5189.
25. Ruddiman WF, McIntyre A (1979) Warmth of the subpolar North Atlantic Ocean during northern hemisphere ice-sheet growth. *Science* 204(4389):173–175.
26. Guihou A, et al. (2011) Enhanced Atlantic Meridional Overturning Circulation supports the last glacial inception. *Quat Sci Rev* 30(13-14):1576–1582.
27. Wang Z, Mysak LA (2002) Simulation of the last glacial inception and rapid ice sheet growth in the McGill Paleoclimate Model. *Geophys Res Lett* 29(23):2102.
28. Govin A, et al. (2012) Persistent influence of ice sheet melting on high northern latitude climate during the early Last Interglacial. *Clim Past* 8(2):483–507.
29. Jochum M, et al. (2012) True to Milankovitch: Glacial inception in the new Community Climate System Model. *J Clim* 25(7):2226–2239.
30. Born A, Nisancioglu K, Braconnot P (2010) Sea ice induced changes in ocean circulation during the Eemian. *Clim Dyn* 35(7):1361–1371.
31. Sarafanov A (2009) On the effect of the North Atlantic Oscillation on temperature and salinity of the subpolar North Atlantic intermediate and deep waters. *ICES J Mar Sci* 66(7):1448–1454.
32. Curry RG, McCartney MS, Joyce TM (1998) Oceanic transport of subpolar climate signals to mid-depth subtropical waters. *Nature* 391(6667):575–577.
33. Hillaire-Marcel C, de Vernal A, Bilodeau G, Weaver AJ (2001) Absence of deep-water formation in the Labrador Sea during the last interglacial period. *Nature* 410(6832): 1073–1077.
34. Thornalley DJR, Elderfield H, McCave IN (2009) Holocene oscillations in temperature and salinity of the surface subpolar North Atlantic. *Nature* 457(7230):711–714.
35. Swift JH, Aagaard K (1981) Seasonal transitions and water mass formation in the Iceland and Greenland seas. *Deep-Sea Res A, Oceanogr Res Pap* 28(10):1107–1129.
36. Ruddiman WF, McIntyre A (1976) Northeast Atlantic paleoclimatic changes over the past 600,000 years. *Geol Soc Am* 145:111–146.
37. Montero-Serrano J-C, Frank N, Colin C, Wienberg C, Eisele M (2011) The climate influence on the mid-depth Northeast Atlantic gyres viewed by cold-water corals. *Geophys Res Lett* 38(19):L19604.
38. Alonso-Garcia M, Sierro FJ, Flores JA (2011) Arctic front shifts in the subpolar North Atlantic during the Mid-Pleistocene (800–400 ka) and their implications for ocean circulation. *Palaeogeogr Palaeoclimatol Palaeoecol* 311(3-4):268–280.
39. McManus JF, Oppo DW, Cullen JL (1999) A 0.5-million-year record of millennial-scale climate variability in the North Atlantic. *Science* 283(5404):971–975.
40. Oppo DW, McManus JF, Cullen JL (2006) Evolution and demise of the Last Interglacial warmth in the subpolar North Atlantic. *Quat Sci Rev* 25(23-24):3268–3277.
41. Bé AWH, Tolderlund DS (1971) Distribution and ecology of living planktonic foraminifera in surface waters of the Atlantic and Indian Oceans. *The Micropaleontology of Oceans*, eds Funnel BM, Riedel WR (Cambridge Univ Press, Cambridge), pp 105–149.
42. Kohfeld KE, Fairbanks RG, Smith SL, Walsh ID (1996) Neogloboquadrina Pachyderma (sinistral coiling) as paleoceanographic tracers in polar oceans: Evidence from northeast water polynya plankton tows, sediment traps, and surface sediments. *Paleoceanography* 11(6):679–699.
43. Pflaumann U, Duprat J, Pujol C, Labeyrie LD (1996) SIMMAX: A modern analog technique to deduce Atlantic sea surface temperatures from planktonic foraminifera in deep-sea sediments. *Paleoceanography* 11(1):15–35.
44. Kipp NG (1976) New transfer function for estimating past sea-surface conditions from sea-bed distribution of planktonic foraminiferal assemblages in the North Atlantic. *Geol Soc Am* 145:3–42.
45. Loubere P (1981) Oceanographic parameters reflected in the seabed distribution of planktic foraminifera from the North Atlantic and Mediterranean Sea. *J Foraminiferal Res* 11(2):137–158.

46. Johannessen T, Jansen E, Flatøy A, Ravelo AC (1994) The relationship between surface water masses, oceanographic fronts and paleoclimatic proxies in surface sediments of Greenland, Iceland, Norwegian Seas. *NATO ASI Ser 1* 17:61–85.
47. Imbrie J, Kipp NG (1971) A new micropaleontological method for paleoclimatology: Application to a Late Pleistocene Caribbean core. *The Late Cenozoic Glacial Ages*, ed Turekian KK (Yale University Press, New Haven), pp 71–91.
48. Darling KF, Kucera M, Kroon D, Wade CM (2006) A resolution for the coiling direction paradox in Neogloboquadrina pachyderma. *Paleoceanography* 21(2):PA2011.
49. Heinrich H (1988) Origin and consequences of cyclic ice rafting in the Northeast Atlantic Ocean during the past 130,000 years. *Quat Res* 29(2):142–152.
50. McManus JF, Anderson RF, Broecker WS, Fleisher MQ, Higgins SM (1998) Radiometrically determined sedimentary fluxes in the sub-polar North Atlantic during the last 140,000 years. *Earth Planet Sci Lett* 155(1-2):29–43.
51. Oppo DW, Horowitz M, Lehman SJ (1997) Marine core evidence for reduced deep water production during termination II followed by a relatively stable substage 5e (Eemian). *Paleoceanography* 12(1):51–63.
52. Oppo DW, Keigwin LD, McManus JF, Cullen JL (2001) Persistent suborbital climate variability in marine isotope stage 5 and termination II. *Paleoceanography* 16(3):280–292.
53. Cannariato KG, Kennett JP (2005) Structure of the penultimate deglaciation along the California margin and implications for Milankovitch theory. *Geology* 33(2):157–160.
54. Cheng H, et al. (2009) Ice age terminations. *Science* 326(5950):248–252.
55. Tzedakis PC, et al. (2012) Can we predict the duration of an interglacial? *Clim Past* 8(5):1473–1485.
56. Simstich J, Sarnthein M, Erlenkeuser H (2003) Paired [delta]18O signals of Neogloboquadrina pachyderma (s) and Turborotalita quinqueloba show thermal stratification structure in Nordic Seas. *Mar Micropaleontol* 48(1-2):107–125.
57. Fronval T, Jansen E, Haflidason H, Sejrup HP (1998) Variability in surface and deep water conditions in the Nordic seas during the last interglacial period. *Quat Sci Rev* 17(9-10):963–985.
58. Galaasen EV, et al. (2014) Rapid reductions in North Atlantic Deep Water during the peak of the last interglacial period. *Science* 343(6175):1129–1132.
59. Irvali N, et al. (2012) Rapid switches in subpolar North Atlantic hydrography and climate during the Last Interglacial (MIS 5e). *Paleoceanography* 27(2):PA2207.
60. Winsor K, Carlson AE, Klinkhammer GP, Stoner JS, Hatfield RG (2012) Evolution of the northeast Labrador Sea during the last interglaciation. *Geochem Geophys Geosyst* 13(11):Q11006.
61. Kandiano ES, Bauch HA, Müller A (2004) Sea surface temperature variability in the North Atlantic during the last two glacial-interglacial cycles: Comparison of faunal, oxygen isotopic, and Mg/Ca-derived records. *Palaeogeogr Palaeoclimatol Palaeoecol* 204(1-2):145–164.
62. Keigwin LD, Curry WB, Lehman SJ, Johnsen S (1994) The role of the deep ocean in North Atlantic climate change between 70 and 130 kyr ago. *Nature* 371(6495):323–326.
63. Adkins JF, Boyle EA, Keigwin L, Cortijo E (1997) Variability of the North Atlantic thermohaline circulation during the last interglacial period. *Nature* 390(6656): 154–156.
64. Bauch HA, Erlenkeuser H (2008) A "critical" climatic evaluation of last interglacial (MIS 5e) records from the Norwegian Sea. *Polar Res* 27(2):135–151.
65. Wang Z, Mysak LA, McManus JF (2002) Response of the thermohaline circulation to cold climates. *Paleoceanography* 17(1):1006.
66. Bond G, et al. (2001) Persistent solar influence on North Atlantic climate during the Holocene. *Science* 294(5549):2130–2136.